Draft version February 1, 2008
Preprint typeset using LaTeX style emulateapj v. 04/03/99

arXiv:astro-ph/0009125v2 12 Dec 2000

# PHOTON CONSUMPTION IN MINIHALOS DURING COSMOLOGICAL REIONIZATION

Zoltán Haiman[1,2,6], Tom Abel[2,3] & Piero Madau[4,5]

[1]Princeton University Observatory, Ivy Lane, Princeton, NJ 08544, USA
[2]Institute for Theoretical Physics, University of California at Santa Barbara, CA 93106, USA
[3]Harvard-Smithsonian Center for Astrophysics, 60 Garden Street MS 10, Cambridge, MA 02138, USA
[4]Institute of Astronomy, Madingley Road, Cambridge, CB3 0HA, U.K.
[5]Department of Astronomy and Astrophysics, University of California, Santa Cruz, CA 95064, USA

*Accepted for publication in ApJ*

## ABSTRACT

At the earliest epochs of structure formation in cold dark matter (CDM) cosmologies, the smallest nonlinear objects are the numerous small halos that condense with virial temperatures below $\sim 10^4$K. Such "minihalos" are not yet resolved in large–scale three–dimensional cosmological simulations. Here we employ a semi–analytic method, combined with three–dimensional simulations of individual minihalos, to examine their importance during cosmological reionization. We show that, depending on when reionization takes place, they potentially play an important role as sinks of ionizing radiation. If reionization occurs at sufficiently high redshifts ($z_r \gtrsim 20$), the intergalactic medium is heated to $\sim 10^4$K and most minihalos never form. On the other hand, if $z_r \lesssim 20$, a significant fraction ( $\gtrsim 10\%$) of all baryons have already collapsed into minihalos, and are subsequently removed from the halos by photoevaporation as the ionizing background flux builds up. We show that this process can require a significant budget of ionizing photons; exceeding the production by a straightforward extrapolation back in time of known quasar and galaxy populations by a factor of up to $\sim 10$ and $\sim 3$, respectively.

*subject headings*: cosmology:theory – early universe – galaxies: evolution

## 1. INTRODUCTION

The lack of any Gunn–Peterson troughs in the spectra of distant quasars (Stern et al. 2000; Fan et al. 2000), as well as the presence of Lyman $\alpha$ emission lines in the spectra of high–redshift galaxies (Weymann et al. 1998; Hu et al. 1999), imply that the hydrogen in the intergalactic medium (IGM) is highly ionized by redshift $z \approx 6$. It is widely believed that reionization was caused by an early population of either galaxies or quasars. The process of reionization and its impact on several key cosmological issues have recently received much theoretical attention, and have been studied by several authors using semi-analytic models (Meiksin & Madau 1993; Shapiro et al. 1994; Haiman & Loeb 1997, 1998) and three–dimensional numerical simulations (Gnedin & Ostriker 1997). In general, these works aim to follow the time evolution of the filling factor of ionized (HII) regions, based on some input prescriptions for the emissivity and spectra of the ionizing sources.

More recent works have focused on the increased rate of recombinations in a clumpy medium relative to a homogeneous one, i.e. when $\langle\rho^2\rangle > \langle\rho\rangle^2$ (Ciardi et al. 2000; Benson et al. 2000; Chiu & Ostriker 2000; Gnedin 2000a; Madau, Haardt, & Rees 1999 [hereafter MHR]). These studies have left significant uncertainties on the details of how reionization proceeds in an inhomogeneous medium. Since the ionizing sources are likely embedded in dense regions, one might expect that these dense regions are ionized first, before the radiation escapes to ionize the low–density IGM. Alternatively, most of the radiation might escape from the local, dense regions along low column density lines of sight. In this case, the underdense 'voids' are ionized first, with the ionization of the denser filaments and halos lagging behind (Miralda-Escudé et al. 2000).

In this paper, we point out that that the density inhomogeneities at the earliest redshifts are dominated by the smallest nonlinear structures, i.e. halos near the cosmological Jeans mass, $M_{\rm Jeans} \approx 10^4$ M$_\odot$. Such small scales have not yet been resolved in numerical simulations of reionization (e.g. Gnedin 2000a), and have also not yet been fully quantified in the semi–analytic works (although see Chiu & Ostriker 2000 and Benson et al. 2000 for partial treatments). Our main goals in this work are (1) to quantify the importance of the high–redshift minihalos as sinks of ionizing photons; and (2) to assess whether by extrapolating to early times the known population of galaxies and quasars a sufficient number of UV photons are produced for hydrogen reionization.

This paper is organized as follows. In § 2, we summarize the ionizing photon budget from the known populations of galaxies and quasars. In § 3, we describe our model of an individual photoevaporating minihalo, based on three–dimensional numerical simulations. Combining this model with a hierarchical structure formation scenario, in § 4 we explicitly show that the ensemble of minihalos dominate the clumping of the high–redshift IGM. In § 5, we then compute the total number of ionizing photons consumed by the photoevaporating minihalos in the same hierarchical cosmology. In § 6, we argue that the minihalos must indeed have been photoevaporated. In § 7, we discuss the

[6]Hubble Fellow.

relevance of the covering factor of minihalos around ionizing sources, and the uncertainties this implies for our results. Finally, in § 8, we offer our conclusions and summarize the implications of this work. Unless mentioned otherwise, throughout this paper we adopt a flat ΛCDM cosmology with $(\Omega_\Lambda, \Omega_b, h, \sigma_8, n) = (0.7, 0.04, 0.7, 0.9, 1)$.

## 2. IONIZING PHOTONS FROM KNOWN SOURCES

The two most natural candidates for reionization are extensions of the known populations of quasars, or of galaxies with ongoing star-formation, to redshifts beyond $z > 6$. Here we briefly review the number of ionizing photons expected from these sources. This will serve as a reference point for comparison to the ionizing photon budget we obtain in our calculations below.

### 2.1. *Quasars*

The luminosity function (LF) of quasars has been measured in optical surveys, and convenient parametric fitting formulae have been published by, e.g. Pei (1995). A more recent determination by the Sloan Digital Sky Survey extends the measurement of the bright end of the LF to higher redshifts, and is consistent with earlier optical results (Fan et al. 2000). Here we adopt the fitting formulae of MHR, which has a somewhat shallower slope towards higher redshifts than, e.g., Pei (1995), and therefore predicts a larger number of quasars when extrapolated to high $z$. We have used this LF, together with the average intrinsic spectrum of Elvis et al. (1995), to compute the production rate of ionizing ($E > 13.6$ eV) photons from quasars. The faint-end slope of the empirical LF is $d\log\Phi/d\log L = -1.64$, so that most ionizing photons are produced by relatively bright quasars near the "knee" of the LF. A recent determination of the high–redshift LF in the soft X–ray band (Miyaji et al. 2000) has yielded significantly weaker evolution out to $z \approx 4.5$ than seen in the optical. Although the X–ray LF still has large uncertainties at $z \gtrsim 2$, taking the X–ray results at face value may indicate the existence of a larger abundance of high–redshift quasars than seen in the optical. If this inference is confirmed in future studies, it could increase the number of ionizing photons produced by bright quasars relative to our estimates below, unless this high–$z$ X–ray population is intrinsically obscured at optical/UV wavelengths.

### 2.2. *Galaxies*

The total star formation rate in the universe can be estimated using the sample of high–redshift galaxies found by the Lyman-break technique (Steidel et al. 1999; Madau & Pozzetti 2000). Since the rest-frame UV continuum at 1500–2800 Å (redshifted into the visible band for distant sources) is dominated by the same short-lived, massive stars which are responsible for the emission of photons shortward of the Lyman edge, the needed conversion factor, about one ionizing photon for every 5 photons at 1500 Å, is fairly insensitive to the assumed IMF and is independent of the galaxy history for $t \gg 10^{7.3}$ yr (MHR). We normalize the number of ionizing photons to the *observed* 1500 Å flux (rest-frame), i.e. bypass the need for any correction due to dust extinction (this is a good approximation provided the mean color excess $E_{912-1500} = 1.6E_{B-V}$ is actually small). We have further assumed an average escape fraction of $f_{esc} = 50\%$ for the ionizing radiation from the galaxy HI layers into the IGM, relative to the escape fraction at 1500 Å. This value is a factor of $\sim 5$ higher than that inferred in nearby starbursts (Leitherer et al. 1995). Theoretically, the escape fraction is expected to be *lower* at high redshifts, because of the higher gas densities then (Wood & Loeb 1999; Dove et al. 2000). However, a recent measurement of the mean escape fraction from a sample of 29 Lyman break galaxies at $\langle z\rangle = 3.4$ has yielded a value $\gtrsim 50\%$ (Steidel et al. 2000). Although the physical implications of this result are still unclear (Haehnelt et al. 2000), to be conservative we adopted this value here.

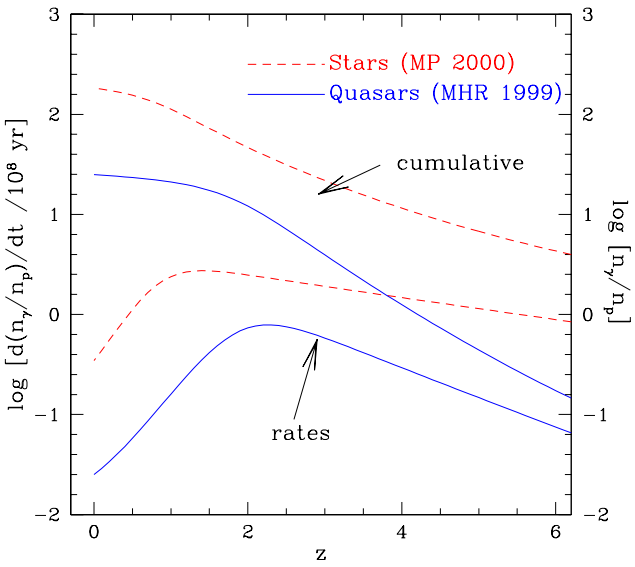


FIG. 1.— Production rate (lower curves) and total number (integrated over cosmic time, starting from high redshift, upper curves) of H-ionizing photons from known quasars and galaxies, extrapolated to $z > 4.5$. The calculations are based on the counts of high–redshift quasars and Lyman break galaxies. We assumed the escape fraction of ionizing photons to be $f_{esc} = 1$ for quasars and $f_{esc} = 0.5 \times f_{esc,1500}$ for galaxies. See text (§ 2) for discussion.

The ionizing photon production rates for both quasars and galaxies are shown in Figure 1, in units of photons above 13.6 eV emitted into the IGM per $10^8$ years per intergalactic hydrogen atom. Also shown is the total number of photons radiated per H-atom prior to redshift $z$. To obtain these integrals, we have extrapolated the photo emission rates $dn_\gamma/dz$ beyond $z = 6$, using the observed slope $d\dot{N}/dz$ at $z = 4$. These extrapolations are clearly very uncertain. For reference, we note that if the photon emission rates had stayed flat at their $z = 6$ values beyond $z > 6$, than in the stellar case, the total number of photons would increase very little ($\approx 20\%$), since the observed rate is already nearly constant in redshift. In the quasar case, this would result in an increase in the total number of photons generated prior to $z = 6$ by a factor of $\approx 4$. Under these extrapolations, as this figure reveals, luminous quasars produce little ionizing radiation prior to redshift $z = 5$, while galaxies provide $\approx 4 \times (f_{esc}/0.5)$ ionizing photons per hydrogen atom by this epoch.

## 3. PHOTOEVAPORATION OF MINIHALOS

In cold dark matter (CDM) cosmologies, the mean density and temperature of the IGM imply the cosmological

Jeans mass of

$$M_{\rm J} \approx 10^4 \left(\frac{\Omega_0 h^2}{0.15}\right)^{-\frac{1}{2}} \left(\frac{\Omega_{\rm b} h^2}{0.02}\right)^{-\frac{3}{5}} \left(\frac{1+z}{11}\right)^{\frac{3}{2}} {\rm M}_\odot, \quad (1)$$

where $M_{\rm J}$ is the total (gas + DM) mass of perturbations allowed to grow in linear theory. This mass corresponds to a virial temperature of the dark matter halo

$$T_{\rm J} \approx 25 \left(\frac{h}{0.7}\right)^{2/3} \left(\frac{\Omega_0 h^2}{0.15}\right)^{-\frac{1}{3}} \left(\frac{\Omega_{\rm b} h^2}{0.02}\right)^{-\frac{2}{5}} \left(\frac{1+z}{11}\right)^{2} {\rm K}. \quad (2)$$

It is natural to expect that the earliest nonlinear objects are hosted in halos of the size described by equations (1) and (2). Numerical simulations find that the mass scale can be up to a factor of $\sim 10$ still lower than this (Gnedin 2000b); however, as we shall find below our results are insensitive to the exact value of the smallest allowed halo size, as long as it is below $T \approx 1000$K. We shall hereafter refer to halos with virial temperatures between $T_{\rm J} \leq T_{\rm vir} \leq 10^4$K as "minihalos". A sufficiently strong early X–ray background (XRB) could catalyze the formation of $H_2$ molecules in minihalos, which could then cool and fragment into stars, or form central black holes (Haiman, Rees & Loeb 1996; Haiman, Abel & Rees 2000). In this case, the gas from the minihalos would likely be ionized and expelled by the *internal* UV source. Alternatively, in the absence of any early XRB, most minihalos would likely not have sufficient molecular abundance to cool and dissipate (Haiman, Rees & Loeb 1997; Haiman, Abel & Rees 2000). In the further absence of any *external* UV radiation, they would then remain in approximate hydrostatic equilibrium until they eventually merge into more massive objects.

However, photoionization by either a nearby external UV source, or by the smooth cosmic UV background radiation after the reionization epoch, heats the gas inside a minihalo to a temperature $\approx 10^4$K. By definition, the gas inside a minihalo is then no longer bound, leading to the photoevaporation of the baryons out of their host halos (Rees 1986; Shapiro, Raga & Mellema 1998; Barkana & Loeb 1999). In general, the resulting photoevaporative outflow has a complex velocity, density and ionization structure, whose time–evolution has been studied in a two–dimensional simulation by Shapiro & Raga (2000). In the present paper, we shall not address this evaporation process itself in detail. Our main goal here is to obtain a rough estimate of how many recombinations each hydrogen atom experiences during the evaporation process. We will therefore use a simplified model of the evaporative flow, which we calibrate using three–dimensional simulations.

### 3.1. *Analytic Model of Photoevaporation*

We begin by adopting a radial density profile $n_{\rm H}(r)$ for the undisturbed gas, based on the spherically symmetric truncated isothermal sphere (TIS, Shapiro, Ilyev & Raga 1999), with the scalings converted to our adopted ΛCDM cosmology as given in Navarro, Frenk & White (1997, hereafter NFW). This profile has the advantage of characterizing a spherical object with a well–defined core, calibrated specifically for use within the Press–Schechter formalism (which we shall use below). For this density profile, the average internal overdensity of the gas within the halo, relative to the background hydrogen density, is $\delta_{\rm int} \equiv \langle n_{\rm H} \rangle / \bar{n}_{\rm H} = 130.5$. Similarly, the mean "internal clumping" is $C_{\rm int} \equiv \langle n_{\rm H}^2 \rangle / \bar{n}_{\rm H}^2 = 444^2$. As an alternative approach, we have assumed the gas to be in hydrostatic equilibrium within a halo that has a density profile as parameterized by NFW, with a concentration parameter $c = 5$. This value was obtained by following the algorithm described in the appendix of NFW, which assigns to each halo of a given mass identified at redshift $z$ a collapse redshift $z_{\rm coll}$ (defined as the time at which half of the mass of the halo was first contained in progenitors more massive that some fixed fraction of the final mass), and assuming that the characteristic halo density is proportional to the critical density at $z_{\rm coll}$ (Navarro, Frenk & White 1997). With this algorithm a minihalo of total mass $M = 10^7\, h^{-1}\, {\rm M}_\odot$ at $z = 10$ has $(z_{\rm coll}, c) = (13.5, 4.8)$ (see also Madau, Ferrara, & Rees 2000). The NFW profile, by definition, has a mean internal overdensity of 200, and the embedded gas is somewhat more centrally condensed than the TIS we adopted, $C_{\rm int} = 532^2$. We conclude that an NFW profile would give similar results to those obtained below, except with the total number of recombinations increased by about $(532/444)^2 \approx 50\%$.

Within the core of the TIS profile, the central density contrast reaches a value as high as $\sim 2 \times 10^4$ relative to the cosmic background. In reality, for gas at temperature $T_{\rm vir}$ that has collapsed adiabatically, the density contrast can not exceed $(T_{\rm vir}/T_{\rm IGM})^{3/2}$, where $T_{\rm IGM}$ is the IGM temperature (given by $T_{\rm IGM}(z) \approx 2.73(1+z_c)[(1+z)/(1+z_c)]^2$ with $z_c \approx 150$). We therefore modify the inner density profile, and adopt $\rho(r) = \min[\rho_{\rm TIS}(r), \rho_{\rm IGM}(T_{\rm vir}/T_{\rm IGM})^{3/2}]$, where $\rho_{\rm TIS}(r)$ is the original TIS density run, and $\rho_{\rm IGM}$ is the density of the uniform IGM. This modification reduces the average density contrast and the internal clumping below their fiducial values of 130.5 and 444 within halos whose virial temperature is lower than $T_{\rm vir} \lesssim 1500$K. Below we find that $\approx 68\%$ of the recombinations in the ensemble of minihalos arise in those with $T_{\rm vir} \lesssim 1500$K, so that uncertainties in the density profiles of the smallest halos do not significantly effect our results.

We next assume that the spherically symmetric halo is suddenly photoionized by an external UV flux. Simultaneously, the gas temperature jumps to $10^4$K, resulting in an outflow. We assume that photoevaporation requires a sound crossing time, $t_{\rm pe} \approx R_{\rm vir}/10$ km s$^{-1}$, so that the photoionized gas retains its original shape for a duration

$$t_{\rm pe} = f \frac{R_{\rm vir}}{10 \text{ km s}^{-1}}, \quad (3)$$

after which it is fully dispersed into the IGM (where $R_{\rm vir}$ is the radius of the TIS). Note that $t_{\rm pe} \propto T_{\rm vir}^{1/2}$, so that smaller halos are photo–dissociated more rapidly. This prescription is admittedly oversimplified, since the gas should expand gradually, and non–uniformly, at varying speeds, rather than as a step–function. In addition, for low UV fluxes, the expansion might start before the gas is ionized (see discussion below). Nevertheless, as we will see below, the numerical simulations show a fairly rapid evaporation, and can be used to calibrate the normalization

constant "$f$" that we have introduced.

### 3.2. *Numerical Simulations*

Our main goal is to estimate the number $N_{\rm pe}$ of recombinations each hydrogen atom experiences during the photoevaporation process. This number is given by

$$N_{\rm pe} = \int dt \int dV x^2 n_{\rm H}^2 \alpha_{\rm B} \times \left[\int dV n_{\rm H}\right]^{-1} = f \frac{R_{\rm vir}}{10 \text{ km s}^{-1}} C_{\rm int} \bar{n}_{\rm H} \alpha_{\rm B} / \delta_{\rm int}. \quad (4)$$

Here the volume integrals are taken over the region that contains the virial gas mass, $x$ is the ionized fraction (which is a function of radius and time), and $\alpha_B = 2.6 \times 10^{-13}$ cm$^3$ s$^{-1}$ is the case B hydrogen recombination coefficient evaluated at $T = 10^4$K. Given an initial density profile, the second line can be readily computed, except for the normalization constant $f$. For reference, we note that the photoevaporation time (eq. 3) for a $T_{\rm vir} = 10^4$K minihalo at redshift $z = 10$ is approximately $25f\%$ of the Hubble time at that redshift; we find that during this interval each hydrogen atom within this halo recombines $N_{\rm pe} = 340f$ times.

The first line in equation (4) is computed explicitly in the simulation, which gives the total number of recombinations each hydrogen atom experienced during the whole photoevaporation process. By comparing this number to the second line, we determine the normalization constant $f$. The simulations are performed by setting up stable truncated isothermal spheres in both dark matter (DM) and gas as the initial condition for the three–dimensional structured adaptive mesh refinement cosmological hydrodynamics code *enzo* of Bryan & Norman (1997; 1999). For simplicity, we use a standard CDM cosmology with $h = 0.5$ and $\Omega_{\rm b} = 0.1$. We solve the chemical reactions for the ions of hydrogen and helium, including collisional ionization, radiative recombinations, and photo–ionization. The reaction rates are taken from Abel et al. (1997). The hydrogen photo–ionization rate is assumed to be uniform on the grid(s); i.e. we do not solve radiative transfer. The photo–ionization heating rate is simply given by $k_{\rm ph}\langle\epsilon_{\rm ph}\rangle$, where $\langle\epsilon_{\rm ph}\rangle$ denotes the average energy of photo–electrons (which depends on the ionizing spectrum; here we adopt $\langle\epsilon_{\rm ph}\rangle = 2$eV).

The typical photoionization rates experienced by minihalos depend strongly on the luminosity and clustering properties of the radiation sources. In addition, the photoionization rates can vary substantially for individual minihalos, because of the $1/r^2$ dependence of the flux from nearby sources. In our simulations, we have experimented with photoionization rates of $k_{\rm ph} = 10^{-13} - 10^{-10}$ s$^{-1}$, corresponding roughly to a background flux of $J = 3\times10^{-23} - 10^{-20}$ erg s$^{-1}$ cm$^{-2}$ Hz$^{-1}$ sr$^{-1}$ at 13.6eV. In general, we find that for fast photoionization rates ($k_{\rm ph} \gtrsim 10^{-12}$ s$^{-1}$), the gas is fully ionized before any motion occurs. In this regime, we find a simple scaling of the numerical results (see below) with halo mass and redshift, independent of the actual value of $k_{\rm ph}$. This is because the heating–induced motions are independent of the photo–heating rate, as long as this rate is comparable to or shorter than the sound crossing time. In the following, we will quote results from simulations with a high–enough flux that allows us to use these scalings, and thus eliminate the need for a large grid of simulations in mass, redshift, and flux.

We emphasize that for smaller UV fluxes, the number of recombinations can be reduced relative to our adopted estimate. The core of the halo has a lower ionization fraction, both because the equilibrium fraction is reduced, and because the photoionization time scale in the core becomes comparable to the sound crossing time (for $k_{\rm ph} \lesssim 10^{-12}$ s$^{-1}$), so that equilibrium is not established before bulk motion occurs. In addition, radiative transfer effects for a low flux might keep the central regions shielded until the density is significantly reduced, and further reduce the number of recombinations. In general, full radiative transfer would be needed to adequately quantify these effects, which we defer to a subsequent paper. Here we only estimate these effects in the optically thin case, and find that for the range of $k_{\rm ph}$ of interest, the reduction in the number of recombinations is small. As an example, for the low rate of $k_{\rm ph} = 10^{-13}$ s$^{-1}$, the core of our fiducial $z = 10$ halo would reach $x = 0.4$, resulting in an overall reduction of the internal clumping of the ionized gas within the halo by a factor of two. Finally, we note that prior to reionization, it is conceivable that, due to the strong fluctuations of the UV flux as a function of position, the gas condenses and photo–evaporates from DM minihalos multiple times, and hence absorb many more photons.

Our calibrations are based on four simulations, using halo masses of $M = 10^6$ M$_\odot$ or $M = 5 \times 10^6$ M$_\odot$; and initial redshifts of $z = 10$ or $z = 20$. In all of these cases, by our choice of the flux, photoevaporation occurs very rapidly, with most recombinations occurring within a sound–crossing time; justifying the assumption of our simple model in equation (3). As an example, in Figure 2 we show the evolution of the $M = 10^6$ M$_\odot$ halo starting at $z = 10$. The figure reveals that by $z = 9.5$ the density contrast is everywhere reduced below $\delta \lesssim 10$. In each of the cases we examined, we infer $f = 1$ from equation (4) to within $\sim 15\%$. For the $M = 10^6$ M$_\odot$ halo, we find $f = 1.03, 0.86$ for $z = 20$ and $z = 10$, respectively. Similarly, for $M = 5 \times 10^6$ M$_\odot$, we find $f = 0.85, 0.89$ for $z = 20$ and $z = 10$. Generally, considerable differences in the inferred values of $f$ can be expected if one were to carry out radiative transfer calculations for more realistic density distributions and source evolutions. In the rest of this paper, we take our four simulations at face value, and set $f = 1$ in the remaining calculations.

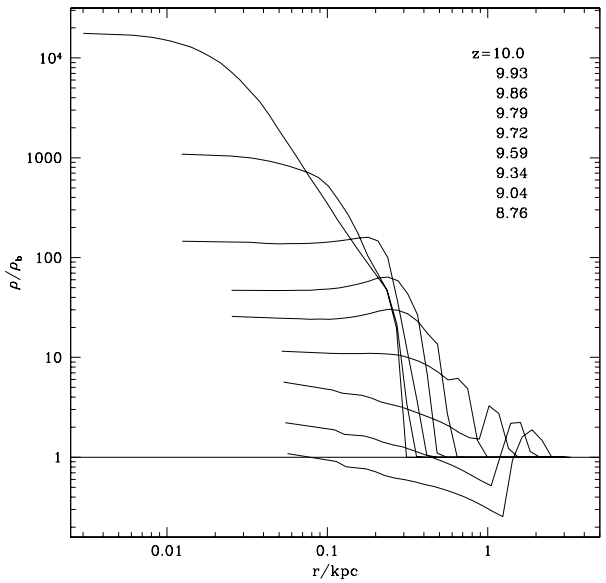


FIG. 2.— The evolution of the density profile of a halo with mass $10^6$ $M_\odot$, illuminated by a background flux at $z = 10$.

## 4. MINIHALOS AND GAS CLUMPING

In this section, we illustrate the importance of minihalos by estimating their contribution to the overall clumpiness of gas in the universe. For simplicity, we assume sudden reionization at some redshift $z_r$, corresponding to the overlap of discrete HII regions, and a sudden increase in the background flux at photon energy $E = 13.6$eV from zero to a value $J = J_{21} \times 10^{-21}$ erg s$^{-1}$ cm$^{-2}$ Hz$^{-1}$ sr$^{-1}$. Prior to $z_r$ the background flux is assumed to be negligible, so that minihalos form down to the Jeans mass, or down to the virial temperature of $T_{\rm J}$ (eq. 2).

At the overlap epoch, the minihalos with $T_{\rm vir} < 10^4$K contain a mass fraction

$$f_M(z_r) = F_{\rm coll}(z_r, T_{\rm J}) - F_{\rm coll}(z_r, 10^4 \text{ K}) \qquad (5)$$

of all baryons, where $F_{\rm coll}(z, T)$ is the Press–Schechter collapsed fraction at redshift $z$ above the mass cutoff corresponding to the virial temperature $T$. The minihalos therefore fill a fraction

$$f_V(z_r) \approx \frac{f_M(z_r)}{130.5} \qquad (6)$$

of the volume, where $\delta_{\rm int} = 130.5$ is the average overdensity within a minihalo relative to the background. The fraction we use in our calculations is somewhat larger than this value because, as discussed in § 3.1. above, we reduce the central densities of the smallest minihalos relative to the TIS model; as a result, they occupy a larger volume.

Once the ionizing flux turns on, the minihalos are photoionized, and each minihalo contributes to the gas clumping and increases the universal mean recombination rate, until it is photoevaporated. To illustrate the importance of minihalos, it is useful to define an average gas clumping factor,

$$C = \frac{\langle n_{\rm H}^2 \rangle}{\bar{n}_{\rm H}^2} = C_{\rm IGM} + C_> + C_<, \qquad (7)$$

where the three terms represent the contributions from the smooth IGM, halos with $T_{\rm vir} > 10^4$K, and minihalos, respectively. Previous works have computed gas clumping in a similar manner, but have not included the contribution $C_<$ from minihalos (see Benson et al. 2000). Each term in equation (7) can be written as $C_i = f_{V,i}\langle n_i^2 \rangle / \bar{n}_{\rm H}^2$, where $f_{V,i}$ is the volume filling factor and $n_i$ is the number density of ionized hydrogen in the $i^{\rm th}$ component. The first term is obtained by assuming that the uncollapsed gas mass fraction $\approx [1 - F_{\rm coll}(z, T_{\rm J})]$ is fully ionized, and uniformly fills the available volume $\approx [1 - F_{\rm coll}(z, T_{\rm J})/130.5]$ (in our calculations, we have included the small correction to these expressions due to the reduction of the central densities of small minihalos). Note that the uncollapsed gas fraction is underdense relative to the overall mean of the universe, so that $C_{\rm IGM} \leq 1$.

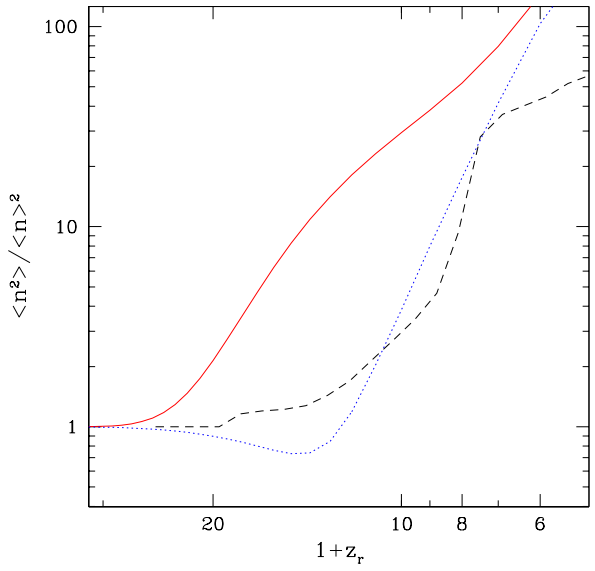


FIG. 3.— Average clumping factor of ionized gas as a function of reionization redshift, when minihalos are included (solid curve), and when only halos with $T_{\rm vir} > 10^4$K are included (dotted curve). The dashed curve is from a hydrodynamical simulation by Gnedin & Ostriker (1997).

The contribution from large halos, $C_>$ is computed by summing over all halos with $T_{\rm vir} > 10^4$K, whose abundance is assumed to follow the Press–Schechter mass function. These halos are collisionally ionized when they virialize, and subsequently cool via atomic line cooling. In the absence of an external UV field, most of the hydrogen would recombine, and remain neutral. When exposed to the photoionizing background, the large halos are self–shielding, and are still only partially ionized from the surface inward. This renders estimates of the contribution from large halos to the overall clumping highly uncertain, since the gas in each halo can continue to cool, self-shield, and collapse to form a disk, while it is being illuminated by the external radiation field. Nevertheless, in order to derive an illustrative estimate, we have computed the radius $r_i$ to which the halos are ionized from the outside in, assuming that the gas density profiles follow that of the TIS solution. We have assumed further that the spherical halo is exposed to an external ionizing flux of $J_{21} = 1$,

and repeated the 1D radiative transfer calculation for several halo masses, to obtain $r_i$ as a function of $M_{\rm halo}$. We then evaluated $\langle n_i^2 \rangle$ for each halo mass, excluding the neutral core $0 < r < r_i$ in each case, and obtained the final clumping factor by averaging $\langle n_i^2 \rangle$ over $M_{\rm halo}$.

Finally, the contribution $C_<$ from minihalos is computed by summing the internal clumping $C_{\rm int} \leq 444^2$ over all minihalos with $T_{\rm J} \leq T_{\rm vir} \leq 10^4$K, assuming that each minihalo is fully ionized, but only exists for a time $t_{\rm pe}$ given by equation (3). To illustrate the importance of minihalos, the resulting clumping factors $C_{\rm IGM} + C_> + C_<$ and $C_{\rm IGM} + C_>$ are shown by the solid and dotted curves in Figure 3, respectively. Also shown for comparison is the clumping factor in a similar ΛCDM cosmology from the numerical simulation of Gnedin & Ostriker (1997, dashed curve). Our calculations show $C$ as a function of the assumed reionization redshift, while the simulation result is adopted from a specific reionization history; this simple comparison is therefore somewhat inappropriate. Nevertheless, as the figure shows, the 3D simulation results are well reproduced by the ensemble of partially ionized spherical halos with $T_{\rm vir} > 10^4$K, assuming a fixed background flux. However, when the minihalos are included, clumping sets in at a significantly higher redshift ($z \approx 20$ instead of $z \approx 10$). Although the relative importance of minihalos decreases at lower redshifts, when larger scales start to collapse, the clumping factor is still enhanced by a factor of $\sim 2$ at $z \approx 6$.

## 5. MINIHALOS AS PHOTON SINKS

We will now explicitly compute the total number of ionizing photons consumed inside minihalos following the overlap epoch $z_r$. This equals the number of recombinations that occur while the gas is evaporated out of the minihalos. Although larger halos with $T_{\rm vir} > 10^4$K eventually dominate the gas clumping, as emphasized in the previous section, large halos can self–shield, cool, and collapse to form disks, making it difficult to estimate their overall contribution. In order to avoid these complications, below we focus on minihalos, and simply ignore halos with $T_{\rm vir} > 10^4$K.

Consider a post–overlap redshift $z < z_r$, with $\Delta t(z, z_r)$ denoting the time elapsed between $z_r$ and $z$. By this redshift, the smallest minihalos have been evaporated, but those with virial temperatures above

$$T_{\rm pe}(z) = 10^4 \left[ \frac{\Delta t(z, z_r)}{t_{\rm pe}(z_r, 10^4{\rm K})} \right]^2 \ {\rm K} \qquad (8)$$

are still present (cf. eq. 3) and are contributing to the gas clumping. The contribution of minihalos to the clumping factor at redshift $z$ is accordingly given by

$$C_<(z) = \int_{M(T_{\rm min})}^{M(10^4{\rm K})} dM \left( \frac{dN}{dM} \right)_{z_r} \left( \frac{M}{\delta_{\rm int} \rho_{\rm bg}} \right) C_{\rm int} \qquad (9)$$

where the first term in the integrand is the Press–Schechter mass function; the second term represents the volume–filling factor of halos of mass $M$; and the last term is the internal gas clumping of a halo of mass $M$, $C_{\rm int}(M) \leq 444$. The lower limit of the integration corresponds to the smallest halo that has not yet been photoevaporated, whose virial temperature is

$$T_{\rm min}(z) = \max(T_{\rm J}, T_{\rm pe}). \qquad (10)$$

Since $T_{\rm J}$ is always evaluated at redshift $z_r$, the only $z$–dependence of equation (9) are through the minimum temperature of minihalos still being evaporated, and through the decrease of the background density $\rho_{\rm bg}$. Some of the minihalos are destroyed by mergers; however, we find from the extended Press–Schechter formalism (Lacey & Cole 1993; eq. 28) that in the relevant ranges of redshifts (corresponding to the photoevaporation time) and halo masses this fraction is always small. The total number of recombinations per hydrogen atom in the universe that takes places in minihalos between $z_r$ and $z$ is then given by

$$N_{\rm rec} = \int_{t(z_r)}^{t(z)} dt \alpha_{\rm B} C_<(z) \bar{n}_{\rm H,0} (1+z)^3, \qquad (11)$$

where $\bar{n}_{\rm H,0}$ is the present–day average density of hydrogen atoms. Figure 4 shows the evolution of $N_{\rm rec}$, assuming different values for the reionization redshift, $6 \leq z_r \leq 16$. In general, the number of recombinations associated with the photoevaporation of minihalos is significant. For popular values for the reionization redshift, the minihalos consume over 10 ionizing photons per hydrogen atom. Most recombinations take place within a short time after reionization – once the minihalos are evaporated, they no longer contribute to recombinations, as demonstrated by the rapid flattening of the curves to their asymptotic values in Figure 4. We recall that smaller halos are photoevaporated more rapidly than larger ones, which makes their importance diminish towards lower masses, despite their increasing abundance. We find that $\approx 68\%$ of the recombinations shown in Figure 4 take place in those with $T_{\rm vir} \lesssim 1500$K; and excluding halos with $T_{\rm vir} < 1000$K would make a negligible difference. Our results imply that if the minihalos were indeed photoevaporated (see discussion below), the ionizing sources must have produced at least $\sim 10$ ionizing photons per background hydrogen atom. This is a necessary, but not a sufficient condition for reionization (e.g. a sudden burst of 10 ionizing photons per H atom could evaporate the minihalos and reionize the universe, but would not ensure that most of the volume is subsequently *kept* ionized).

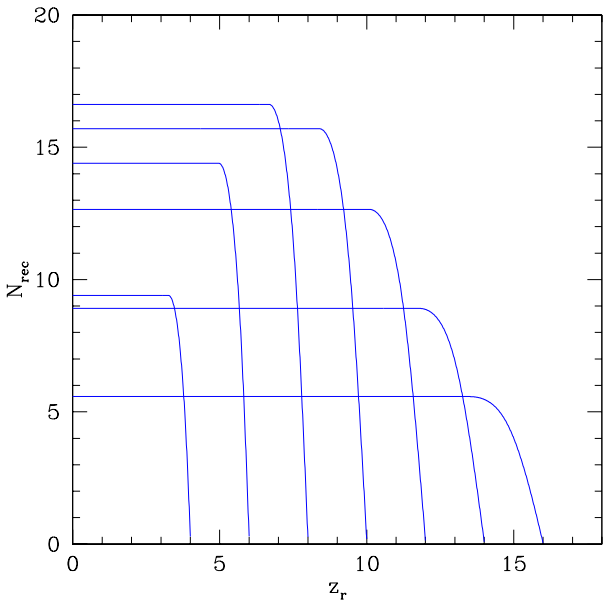


FIG. 4.— Total number of recombinations inside minihalos, following sudden reionization at redshift $z_r$. Recombinations are shown per hydrogen atom, assuming the mean IGM density (see eq. 11).

An interesting feature in Figure 4 is the dependence of the number of recombinations on the assumed reionization redshift. If reionization occurs early ($z_r \gtrsim 20$), i.e. by efficient ionizing photon production in rare, high–$\sigma$ objects, the abundance of minihalos is then still low. Since we do not allow minihalos to condense after reionization, most minihalos never form. As a result, minihalos are less important sinks of ionizing radiation. Likewise, if reionization occurs late (closer to $z = 6$), then the minihalos have started merging into larger halos with $T_{\rm vir} > 10^4$K. In this case, a fraction of minihalos reside in deep potential wells and can be self–shielded, reducing their role as photon sinks. The effect of minihalos are maximal if reionization occurs around the popular values of $z \approx 8 - 10$, the redshift when the minihalo abundance also peaks (note that this redshift depends sensitively on the assumed cosmology, and on the normalization of the power spectrum $\sigma_8$).

In our treatment, we assumed sudden reionization. The later stages of reionization, corresponding to the slow outside–in ionization of dense regions on larger scales, can last a considerable fraction of the Hubble time. However, the initial overlap of HII regions likely proceeds rapidly (Haiman & Loeb 1998; Miralda-Escudé et al. 1999; MHR; Gnedin 2000a). Nevertheless, one could follow the volume filling factor of ionized regions, and allow the formation of new minihalos only outside these regions (as is done in Haiman & Loeb 1998). Here we simply note that if the overlap epoch lasts between redshifts $z_1$ and $z_2$, then reading $N_{\rm rec}$ from Fig 4 at these two redshifts would approximately bracket the number of photons consumed.

## 6. THE MEAN FREE PATH OF IONIZING PHOTONS

The minihalos that formed prior to the reionization redshift $z_r$ contribute to the Lyman-continuum opacity of the universe and reduce the mean free path of ionizing photons at later redshifts $z < z_r$. No new minihalos form after reionization, and furthermore, a fraction $1 - f_{\rm surv}$ of the existing minihalos disappear by merging, as they become parts of larger halos. Assuming the minihalos to be neutral and randomly distributed in space, the comoving photon mean free path $d$ at redshift $z$ is given by

$$\frac{1+z}{d} = \int_{M_{\rm J}}^{M_0} dM\ n(M,z)\sigma(M) f_{\rm surv}(M, z_r, M_0, z) = \int_{M_{\rm J}}^{M_0} dM \left(\frac{dN}{dM}\right)_{z_r} (1+z)^3 (\pi R_{\rm vir}^2) f_{\rm surv}, \quad (12)$$

where $\sigma(M)$ is the geometrical cross–section, $R_{\rm vir}$ is the virial radius, $n(M, z)$ is the physical abundance at redshift $z$, and $(dN/dM)_{z_r}$ is the comoving abundance at redshift $z_r$ of minihalos of mass $M$; and $f_{\rm surv}(M, z_r, M_0, z)$ is the probability that a halo of mass $M$ at redshift $z_r$ has not become part of a halo of mass $> M_0$ by redshift $z$. Here and in the upper limit of the integrals in equation (12), $M_0$ is chosen to correspond to a virial temperature of $10^4$K. The survival fraction is computed as

$$f_{\rm surv}(M, z_r, M_0, z) = 1 - \int_{M_0}^{\infty} dM_1 p(M, z_r, M_1, z), \quad (13)$$

where $p(M, z_r, M_1, z)$ is the probability that a halo of mass $M$ at redshift $z_r$ is part of a halo of mass $M_1 \pm dM_1/2$ at redshift $z$, given by Lacey & Cole (1993, eq. 28).

We find that the mean free path is small compared to the Hubble distance $ct_{\rm Hub}(z)$. For example, taking $z_r = 10$ as the reionization redshift, we find $d = 2.1$(comoving) Mpc at $z = 10$. Equation (12) also shows that the contribution to the opacity from halos of mass $M$ scales approximately as $\propto M^{-1/3}$, implying that once the low–density IGM is ionized, but the halos are still neutral, the minihalos are the dominant source of opacity. *As a result, the typical fate of an ionizing photon emitted around redshift $z \approx 10$ is to be absorbed by a minihalo within a small fraction of the Hubble distance.*

Although most ionizing photons are absorbed by minihalos, it is interesting to follow the evolution of the mean free path at $z < z_r$ under the assumption that the minihalos stay neutral. This could be the case, e.g. if only $\sim$ one ionizing photon is produced in the universe per H atom after $z_r$. We find that approximately half of the minihalos present at $z = 10$ survive merging into large halos until $z = 3$, and the surviving minihalos lead to mean free paths of $d = 10, 16$, and 32 Mpc at $z = 5, 4$, and 3, respectively. This implies the existence of $dN/dz \approx 54, 42$, and 31 minihalos per unit redshift at these redshifts. The minihalos considered here have hydrogen column densities of $N_{\rm H} \gtrsim 10^{18}$ cm$^{-2}$, and their abundances should therefore be compared to that of high–redshift Lyman limit systems (LLS). Although the latter is not well measured at $z \approx 5$, it is inferred from high–resolution quasar spectra to be $dN/dz \approx 2 \pm 0.5$ at $z = 3$ and $dN/dz \approx 3.5 \pm 1$ at $z = 4$ (e.g. Storrie-Lombardi et al. 1994), at least a factor of $\sim 10$ lower than the number of surviving minihalos. We conclude that the observed relatively low number of LLS gives a strong constraint on the number of minihalos that could have survived photoevaporation. Unless future observations reveal a 10–fold increase in the abundance of Lyman limit systems from $z = 4$ to $z = 5$, this provides

strong evidence that most minihalos were indeed photoevaporated by $z \approx 5$ (or at least their total geometrical cross–sections were reduced by an order of magnitude). Indeed, Abel & Mo (1998) have shown that halos with $T_{\rm vir} \gtrsim 10^4$K already have a sufficient abundance to account for all LLS at $z \lesssim 4$; leaving no room for additional minihalos.

## 7. THE COVERING FACTOR OF MINIHALOS

So far we have assumed that reionization occurs suddenly. Stated more precisely, in this picture reionization occurs in three stages. First, the HII regions around individual ionizing sources rapidly overlap and fill most of the volume, occupied by the low–density IGM. Second, the minihalos are photoevaporated by the background radiation. Finally, the larger–scale dense regions are gradually ionized from the outside inwards. This scenario is justified as long as the minihalos have a small covering factor $F_{\rm cov}$ around an ionizing source. Here $F_{\rm cov}$ is defined as the fraction of the $4\pi$ solid angle around a typical ionizing source occupied by minihalos out to a distance $r_s$, where $r_s$ is the typical separation of the ionizing sources. On the other hand, if $F_{\rm cov} \gtrsim 1$, then the minihalos *must be* photoevaporated before the low–density regions can be ionized, since ionizing photons are necessarily absorbed in minihalos before they are able to reach most of the volume. In this case, the first two stages of reionization would be reversed, and a typical minihalo is evaporated by a neighboring UV source, rather than by a uniform background. The resulting "lopsided" photoevaporation is considerably more complicated to model than the evaporation by a uniform background, as we assumed in § 3. Although such modeling is beyond the scope of the present paper, we shall estimate the covering factor below.

To estimate the covering factor, let us assume that the ionizing sources reside in halos with virial temperatures $T_{\rm vir} \approx 10^4$K, or mass $M_0$. Taking $z_r = 10$, the average separation of these sources at the reionization epoch is $r_s = [M_0(dN/dM_0)]^{-1/3} = 0.5$ (comoving) Mpc. If the minihalos were randomly distributed, $F_{\rm cov}$ could be computed analogously to the mean free path (cf. eq. 12), and would be given simply by

$$F_{\rm cov,0} = \frac{r_s}{d} \approx \frac{0.5}{2.1} \approx 25\%. \qquad (14)$$

However, equation (14) ignores the fact that minihalos are strongly clustered around the ionizing sources, and therefore cover a larger fraction of the sky. Taking clustering into account, the abundance of minihalos of mass $M_1$ at a distance $r \pm dr$ away from an ionizing source in a halo of mass $M_0$ is given approximately by

$$N \approx N_1[1 + b_0 b_1 \xi_m(r)], \qquad (15)$$

where $N_1 = M_1(dN/dM_1)$ is the average minihalo abundance, $\xi_m(r)$ is the mass correlation function at redshift $z = 10$, and $b_1 = b(z_r, M_1)$ and $b_0 = b(z_r, M_0)$ are the bias of halos of mass $M_1$ and $M_0$ relative to mass. The smallest spatial scale we consider is the virial radius of a halo at the Jeans mass, $\approx 1$ (comoving) kpc, which is in the mildly non-linear regime. For simplicity, we use the linear correlation function and halo bias, although nonlinear effects could increase the clustering somewhat above the estimates below. The relevant halo masses are always above $M^*$, i.e. even the smallest minihalo has a positive bias parameter $b(z, M)$.

For halos of a given mass $M_1$, clustering then increases the covering factor to

$$F_{\rm cov} = F_{\rm cov,0}[1 + \frac{b_0 b_1}{r_s} \int_{R_{\rm vir}}^{r_s} dr \xi_m(r)]. \qquad (16)$$

Here $R_{\rm vir}$ refers to the virial radius of the minihalo of mass $M_1$. Averaging the term in square brackets over all masses between $M_{\rm J}$ and $M_0$, we find that the overall increase at redshift $z = 10$ is a factor of $\approx 3$. The mass-dependence is primarily through the bias parameter $b_1$, since the linear mass correlation function $\xi_m(r)$ is quite flat, and the radial integral is dominated by large radii.

In summary, our estimates imply a typical covering factor of $F_{\rm cov} \approx 75\%$. This relatively large value demonstrates that most ionizing photons emitted by a source are absorbed in minihalos before most of the volume of the IGM can be ionized. Our estimates are inherently uncertain, as they are based on spherical halos and the linear correlation functions. As higher resolution three–dimensional simulations become feasible in the future, it will possible to directly compute the covering factor of minihalos, and eventually to model their asymmetric photoevaporation (as done in two dimensions by Shapiro & Raga 2000).

## 8. CONCLUSIONS

We have shown that minihalos, i.e. halos with virial temperatures between the cosmological Jeans temperature, $T_{\rm J}$, and $10^4$K, play an important role during cosmological reionization. In the earliest stages of reionization, the minihalos dominate the average gas clumping in the universe, and can therefore dominate the overall recombination rate. Depending on the reionization redshift, up to $\approx 20\%$ of all baryons condense into minihalos before their formation is suppressed by the reheating feedback. The fate of the chemically pristine minihalos depends on the abundance of $H_2$ molecules (see Haiman, Abel & Rees 2000). A sufficiently strong early X–ray background (XRB) could catalyze the formation of $H_2$ molecules, and the minihalos could then cool and harbor internal ionizing sources, likely photo–evaporating their gas content from the inside (note that X–rays would have several additional important consequences for reionization, see Oh 2000). In absence of any early XRB, however, most minihalos would likely not have sufficient molecular abundance, and they would then remain in approximate hydrostatic equilibrium until photoevaporated by external ionizing sources.

We find that the photoevaporation of existing minihalos in the range of virial temperatures 1000 K $\lesssim T_{\rm vir} \lesssim 10^4$ K dominates the necessary ionizing photon budget, and requires $10 - 20$ ionizing photons per background hydrogen atom. This value exceeds by about an order of magnitude the number of ionizing photons produced by an extrapolation of known populations of quasars to higher redshifts. An extrapolation of the Lyman break galaxy population to high redshift comes closer to meeting the required photon budget, provided that a large fraction of the ionizing photons produced in these galaxies leak into the IGM. If the mean escape fraction is $\sim 50\%$ (cf. Steidel et al. 2000),

then the discrepancy is only a factor of $\sim 3$. Our conclusions depend further on the type of sources responsible for reionization. Our results show that if the reionizing sources have typical separations of halos with virial temperatures of $10^4$K (or larger), then most minihalos are photoevaporated before most of the volume of the universe is reionized, because their covering factor around the ionizing sources is of order unity. If the reionizing sources are more closely packed, in principle they could ionize the low–density regions, i.e. most of the volume, before the minihalos are photoevaporated. In either case, we find that the minihalos must have been photoevaporated by $z \approx 5$, in order not to overpredict the number of Lyman limit systems by a factor of $\sim 10$.

In a previous study of inhomogeneous reionization, Miralda-Escudé et al. (2000) have suggested that $\sim$ one ionizing photon per hydrogen atom is sufficient to reionize most of the volume of the IGM by $z \approx 5$. The gas clumping in that study was adjusted to match the results of numerical simulations, which did not resolve the smallest scales, i.e. scales on which minihalos dominate the gas clumping. Our results suggest that the necessary photoevaporation of dense gas out of minihalos can raise the photon requirement at $z \gtrsim 5$ by up to an order of magnitude. In arriving at this conclusion, we have relied on a combination of a semi–analytic approach and three-dimensional simulations of individual halos, albeit without radiative transfer, and we have also made a number of simplifying assumptions. More realistic cosmological hydrodynamical simulations that include realistic sources and three–dimensional radiative transfer will be available in the near future, and will be able to test our simplified model.

The additional ionizing photons required for the photoevaporation of minihalos could arise from an early population of low–luminosity quasars ("miniquasars"), whose abundance declines significantly less than that of optically bright QSOs. Alternatively, ionizing photons could have been produced in "minigalaxies" associated with low–mass halos collapsing at high redshift. Although both types of sources could have escaped detection with present instruments, both are well within the capabilities of direct imaging with future telescopes, such as the *Next Generation Space Telescope*.

We thank Houjun Mo for useful discussions, and Jordi Miralda-Escudé, Martin Haehnelt, Martin Rees, Rennan Barkana, and the referee, David Weinberg, for useful comments on the manuscript. We also thank Greg Bryan and Mike Norman for permission to use their adaptive mesh refinement code *enzo*. This research was supported by the NSF under Grant No. PHY94-07194 at the ITP, and by NASA through the Hubble Fellowship grant HF-01119.01-99A, awarded to ZH by the Space Telescope Science Institute, which is operated by the Association of Universities for Research in Astronomy, Inc., for NASA under contract NAS 5-26555. PM acknowledges support by NASA through ATP grant NAG5–4236.

REFERENCES

Abel, T., Anninos, P., Zhang, Y., & Norman, M. L. 1997, New Ast, 2, 181
Abel, T., & Mo, H. J. 1998, ApJ, 494, L151
Barkana, R., & Loeb, A. 1999, ApJ, 523, 54
Benson, A. J., Nusser, A., Sugiyama, N., & Lacey, C. G. 2000, MNRAS, in press, astro-ph/0002457
Bryan, G. L., & Norman, M. L. 1997, in Computational Astrophysics, ASP Conf. Ser. No. 123, eds. D.A. Clarke and M. Fall
Bryan, G. L., & Norman, M. L. 1999, in Workshop on Structured Adaptive Mesh Refinement Techniques, ed. N. Chrisosoides, p. 167
Chiu, W. A., & Ostriker, J. P. 2000, ApJ, 534, 507
Ciardi, B., Ferrara, A., Governato, F., & Jenkins, A. 2000, MNRAS, 314, 611
Dove, J. B., Shull, J. M., & Ferrara, A. 2000, ApJ, 531, 846
Elvis, M., Wilkes, B. J., McDowell, J. C., Green, R. F., Bechtold, J., Willner, S. P., Oey, M. S., Polomski, E., & Cutri, R. 1994, ApJS, 95, 1
Fan, X. etal. 2000, AJ, in press, astro-ph/0005414
Gnedin, N. Y. 2000a, ApJ, 535, 530
Gnedin, N. Y. 2000b, ApJ, 542, 535
Gnedin, N. Y., & Ostriker, J. P. 1997, ApJ, 486, 581
Haehnelt, M. G., Madau, P., Kudritzki, R., & Haardt, F. 2000,ApJ, submitted, astro-ph/0010631
Haiman, Z., Abel, T., & Rees, M. J. 2000, ApJ, 534, 11
Haiman, Z., & Loeb, A. 1997, ApJ, 483, 21
Haiman, Z., & Loeb, A. 1998, ApJ, 503, 505
Haiman, Z., Rees, M. J., & Loeb, A. 1996, ApJ, 467, 522
Haiman, Z., Rees, M. J., & Loeb, A. 1997, ApJ, 476, 458
Hu, E. M., McMahon, R. G., & Cowie, L. L. 1999, ApJ, 522, L9
Lacey, C., & Cole, S. 1993, MNRAS, 262, 627
Leitherer, C., Ferguson, H. C., Heckman, T. M., & Lowenthal, J. D. 1995, ApJ, 454, L19
Madau, P., Ferrara, A., & Rees 2000, ApJ, submitted, astro-ph/0010158
Madau, P., Haardt, F., & Rees, M. J. 1999, ApJ, 514, 648 [MHR]
Madau, P., & Pozzetti, L. 2000, MNRAS, 312, 9
Meiksin, A., & Madau, P. 1993, ApJ, 412, 34
Miralda-Escudé, J., Haehnelt, M., & Rees, M. J. 2000, ApJ, 530, 1
Miyaji, T., Hasinger, G., & Schmidt, M. 2000, A&A, 353, 25
Mo, H.J., Mao, S. & White, S.D.M. 1998, MNRAS, 295, 319
Navarro, J. F., Frenk, C. S., & White, S. D. M. 1997, ApJ, 490, 493 (NFW)
Oh, S. P. 2000, ApJ, submitted, astro-ph/0005262
Pei, Y. C. 1995, ApJ, 438, 623
Press, W. H., & Schechter, P. L. 1974, ApJ, 181, 425
Rees, M. J. 1986, MNRAS, 218, 25p
Shapiro, P. R., Giroux, M. L., & Babul, A. 1994, ApJ, 427, 25
Shapiro, P. R., Ilyev, I., & Raga, A. C. 1999, MNRAS, 307, 203
Shapiro, P. R., & Raga, A. C. 2000, in Cosmic Evolution and Galaxy Formation: Structure, Interactions, and Feedback, ASP Conference Series, eds. J. Franco, E. Terlevich, O. Lopez-Cruz, I. Aretxaga, in press, astro-ph/0004413
Shapiro, P. R., Raga, A. C., & Mellema, G. 1998, in Molecular Hydrogen in the Early Universe, Memorie Della Societa Astronomica Italiana, Vol. 69, ed. E. Corbelli, D. Galli, and F. Palla (Florence: Soc. Ast. Italiana), p. 463
Steidel, C. C., Adelberger, K. L., Giavalisco, M., Dickinson, M., Pettini, M. 1999, ApJ, 519, 1
Steidel, C. C., Pettini, M., & Adelberger, K. L. 2000, ApJ, in press, astro-ph/0008283
Stern, D., Spinrad, H., Eisenhardt, P., Bunker, A. J., Dawson, S., Stanford, S. A., Elston R. 2000, ApJL, 533, 75
Storrie-Lombardie, L. J., McMahon, R. G., Irwin, M. J., & Hazard, C. 1994, ApJ, 474, L13
Weymann, R. J., Stern, D., Bunker, A., Spinrad, H., Chaffee, F. H., Thompson, R. I., & Storrie-Lombardi, L. J. 1998, ApJ, 505, 95
Wood, K. & Loeb, A. 1999, ApJ, submitted, astro-ph/9911316